



Contents lists available at ScienceDirect

Journal of the European Ceramic Society

journal homepage: www.elsevier.com/locate/jeurceramsoc

Short communication

A five-component entropy-stabilized fluorite oxide

Kepi Chen^{a,*}, Xintong Pei^a, Lei Tang^a, Haoran Cheng^a, Zemin Li^a, Cuiwei Li^b, Xiaowen Zhang^c, Linan An^d^a School of Energy, Power and Mechanical Engineering, North China Electric Power University, Beijing, 102206, China^b School of Mechanical, Electronic and Control Engineering, Beijing Jiaotong University, Beijing, 100044, China^c School of Materials Science and Engineering, Tsinghua University, Beijing, 10083, China^d Department of Materials Science and Engineering, University of Central Florida, Orlando, FL 32816, USA

ARTICLE INFO

Keywords:

Entropy-stabilization
Fluorite oxide
Phase transition
Thermal conductivity

ABSTRACT

In this paper, we report a new entropy-stabilized fluorite oxide, formed by solid-state reacting the equimolar mixture of CeO₂, ZrO₂, HfO₂, TiO₂ and SnO₂ at 1500 °C. We demonstrated that the oxide is truly entropy-stabilized by showing that the oxide was transferred to a multiphase state when annealed at lower temperatures, and the transition between the low-temperature multiphase and high-temperature single-phase states is reversible. Room-temperature thermal conductivity of the fluorite oxide was measured to be 1.28 Wm⁻¹ K⁻¹. The value is only half of that for 7 wt% yttria-stabilized zirconia, suggesting the material could be useful for thermal-insulation applications.

1. Introduction

In the past ten years, a new class of materials consisting of five or more elemental species, referred to as high-entropy alloys (HEAs), has attracted extensive attentions [1–6]. In these materials, configurational entropy, instead of cohesive energy, predominates the thermodynamic stability. The concept was inspired by an “accident” discovered during searching for metallic materials with high glass-forming ability. The original hypothesis was that the vitrified ability of a material should be synchronous with its entropy since the amorphous structure is highly disordered (high entropy). However, it was found that vitrified ability was not always coordinated with entropy. Instead, some systems with high configurational entropy can form stable single-phase crystals rather than glasses. It was demonstrated that HEAs exhibited many attractive properties as compared to conventional alloys, such as high hardness, great mechanical strength, and good wear/corrosion resistance. HEAs are becoming a new research focus in the field of materials science and solid-state physics [3–6].

While previous research on high-entropy materials primarily focused on metals, the concept was also explored for non-metallic materials. In 2015, Rost and co-workers successfully synthesized a single-phased (Mg_{0.2}Co_{0.2}Ni_{0.2}Zn_{0.2}Cu_{0.2})O and demonstrated that the rock-salt-structured five-component oxide was stabilized by configurational entropy, thus named it as entropy-stabilized oxide (ESO) [7]. This work represents a breakthrough in searching for high-entropy non-metallic materials. From then onwards, many high-entropy ceramics with

different crystal structures have been realized, including perovskite oxide [8,9], ultrahigh-temperature boride [10], fluorite oxide [11,12] and spinel oxide [13]. It is worth mentioning that although the terms of high-entropy and entropy-stabilization are often used interchangeably by researchers, they refer fundamentally different concepts. High-entropy simply means that the system has high configurational entropy. On the other hand, entropy-stabilization requires that the system has both high configurational entropy and positive forming heat (+ΔH), so that it is entropy that predominates the thermodynamic stability. In fact, many high-entropy materials reported previously are lack of demonstrating the second requirement. That is a reason why HEAs has now been referred to as multiple-principle-element alloys (MPEAs) or complex concentrated alloys (CCAs).

In this paper, we report a new entropy-stabilized fluorite oxide - (Ce_{0.2}Zr_{0.2}Hf_{0.2}Sn_{0.2}Ti_{0.2})O₂. We demonstrate that this five-component oxide can reversibly transform between low-temperature multiphase and high-temperature single-phase, clearly indicating that the single-phase oxide formed at the finite temperature is entropy-stabilized.

2. Experimental

By considering the guidelines for forming entropy-stabilized oxides outlined in ref 7, five-component CeO₂-ZrO₂-HfO₂-SnO₂-TiO₂ system was selected in this study. The crystal structure, coordination number (CN) of cation, and cation radius of these oxides are listed in Table 1. It is seen that CeO₂, ZrO₂ and HfO₂ exhibit fluorite structure, while SnO₂

* Corresponding author.

E-mail address: ckp@ncepu.edu.cn (K. Chen).<https://doi.org/10.1016/j.jeurceramsoc.2018.04.063>Received 13 February 2018; Received in revised form 24 April 2018; Accepted 29 April 2018
0955-2219/ © 2018 Elsevier Ltd. All rights reserved.

Table 1

Crystal structure, cation coordination number and cation radius of the starting oxides.

Oxide	Structure	Cation coordination number	Cation radius (nm)
CeO ₂	Fluorite	8	0.097
ZrO ₂	Fluorite	8	0.084
HfO ₂	Fluorite	8	0.083
SnO ₂	Rutile	6	0.069*
TiO ₂	Rutile	6	0.061*

* The radius of Sn⁴⁺ and Ti⁴⁺ are 0.081 and 0.074 nm, respectively, when their coordination number is 8.

and TiO₂ exhibit rutile structure. The cations have the same valence number, but different radii and CNs.

The synthesis processing is as follows. First, the powders obtained were weighed and ball-milling using alcohol as milling media to form an equimolar mixture. Ball-milling was performed for 6 h to ensure uniform mixing. After that, the mixture was dried and subsequently pre-sintered at 1300 °C for 6 h. The pre-sintered powder was ball-milled again for another 6 h. The resultant powder was pressed into discs of 10 mm diameter and 1 mm thick, which were finally sintered at 1500 °C for 6 h followed by cooling down with furnace. Approximately, it took about 12 min for cooling from 1500 to 1100 °C, which corresponding to a cooling rate of ~33 °C/min.

The phase composition was analyzed using X-ray diffraction (XRD, D8 ADVANCE A25, Bruker). A step size of 0.02° and a collection time of 0.2 s or 3 s per step at 40 kV and 40 mA over the diffraction angle (2θ) ranging from 10 to 80° were used. The microstructure was observed by high-resolution transmission electron microscopy (HR-TEM, JEM-2100F, JEOL). The elemental composition was determined using energy dispersive spectroscopy (EDS) on a field emission scanning electron microscope (FESEM, Quanta FEG 650, FEI) equipped with Oxford Instruments EDS X-Ray spectrometer.

The electric conductivity was measured on a source-meter (2450, Keithley Instruments Inc.) in a temperature range of 600–1100 °C. The thermal conductivity was measured at room temperature using the physical property measurement system (PPMS, 6000, Quantum Design Inc.). The size of sample for thermal conductivity measurement is 5 mm × 5 mm × 3 mm.

3. Results and discussion

The effect of sintering temperature on the phase composition was studied first. It is found that the material was transferred to almost single fluoride phase only when the sintering temperature reached 1500 °C. Fig. 1 is the XRD pattern of the sample sintered at 1500 °C, together with Rietveld analysis. The pattern shows that the sample is almost a pure fluoride phase, with a slight amount of second phase.

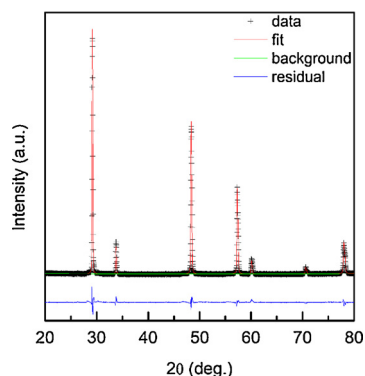


Fig. 1. XRD patterns together with Rietveld fits of the (Ce_{0.2}Zr_{0.2}Hf_{0.2}Sn_{0.2}Ti_{0.2})O₂ sample prepared at 1500 °C.

Lattice parameter calculated from the pattern is 5.3518 Å. This value is smaller than that (5.411 Å) of CeO₂, likely due to that all of the radii of the rest cations are slightly smaller than that of Ce⁴⁺ (Table 1). The (Ce_{0.2}Zr_{0.2}Hf_{0.2}Sn_{0.2}Ti_{0.2})O₂ sample sintered at 1500 °C was also analyzed using TEM. All regions investigated by TEM exhibited perfect crystallinity, evident by the sharp lattice fringes (Fig. 2a and c). The SAED patterns (Fig. 2b and d) have been indexed to be a FCC cubic fluorite (Fm-3m) structure, consistent with XRD findings.

In order to demonstrate the oxide formed above is predominantly stabilized by entropy, we need to show that it can transfer to a multiphase state by annealing at lower temperatures, and the multiphase state can be reversibly transferred back to the original single-phase state by annealing at higher temperatures. To do so, we first annealed the obtained single-phase oxide at different temperatures for 4 h to check whether the single-phase oxide can be transferred to a multiphase one or not. The XRD diffraction patterns of the samples annealed at different temperatures are shown in Fig. 3. It is seen that the new diffraction peaks start to appear when the annealing temperature reaches 1050 °C, indicating the formation of a second phase. The intensity of these new peaks increases when the annealing temperature was increased to 1100 °C. The XRD patterns obtained from the samples annealed at 1000 °C or lower did not show any new diffraction peaks. This could be due to that the concentration of the second phase is too small to be detected or the material remained the single phase.

We then annealed the multiphase oxide obtained at 1100 °C at higher temperatures for 4 h to check if the multiphase state can be transferred back to its original single-phase state or not. Fig. 4 shows the XRD diffraction patterns of the annealed samples. It is seen that the intensity of the diffraction peaks from the sample annealed at 1200 °C are similar to that annealed at 1100 °C, suggesting that the multiphase state is stable within this temperature range. Further increasing the annealing temperature leads to the decrease in the intensity of the diffraction peaks of the second phase. At 1500 °C, the diffraction peaks from the second phase disappeared in XRD profile and the material was transferred back to the original single fluorite phase.

The phase-transition can also be seen from SEM observation on the microstructure. As shown in Fig. 5, compared to the sample sintered at 1500 °C (Fig. 5a), the sample annealed at 1100 °C (Fig. 5b) exhibited the phase decomposition and formation of the second phase. Such phase-decomposition was removed and the microstructure was restored by annealing the sample at 1500 °C again (Fig. 5c).

The above results clearly demonstrate that single fluorite phase formed at 1500 °C is stabilized by configurational entropy. The appearance transition temperature between the multiphase and single-phase states is about 1500 °C. This temperature is much higher than that of the five-component rocksalt oxide reported in Ref. [7]. Note that the maximum configurational entropy for the two oxides should be the same since both of them are equimolar five-component system. Thereby, the significant difference in the phase-transition temperature indicates that the fluorite reported here should have higher positive formation enthalpy.

Further characterization of the oxide obtained at 1500 °C was done by elemental analysis. As shown in Fig. 6, all elements are homogeneously distributed within the material, excepting that Ce exhibits clearly segregation around pores. Such segregation was not detected from XRD analysis, suggesting the amount of segregation is very small. The reason for the formation of such segregation is not clear at this moment. One possible reason is that a small amount of liquid phase was formed during the high temperature sintering. The miscibility gap between the solid phase and the liquid phase can lead to elemental segregation, which has been commonly observed in liquid phase sintered ceramics. Another possible reason could be that the solid solution is not an ideal regular solid solution where atoms are distributed randomly, but a sub-regular solid solution. In sub-regular solid solutions, Gibbs free energy-composition curve is not symmetric, which can also lead to phase separation (or elemental segregation) [15]. Complex

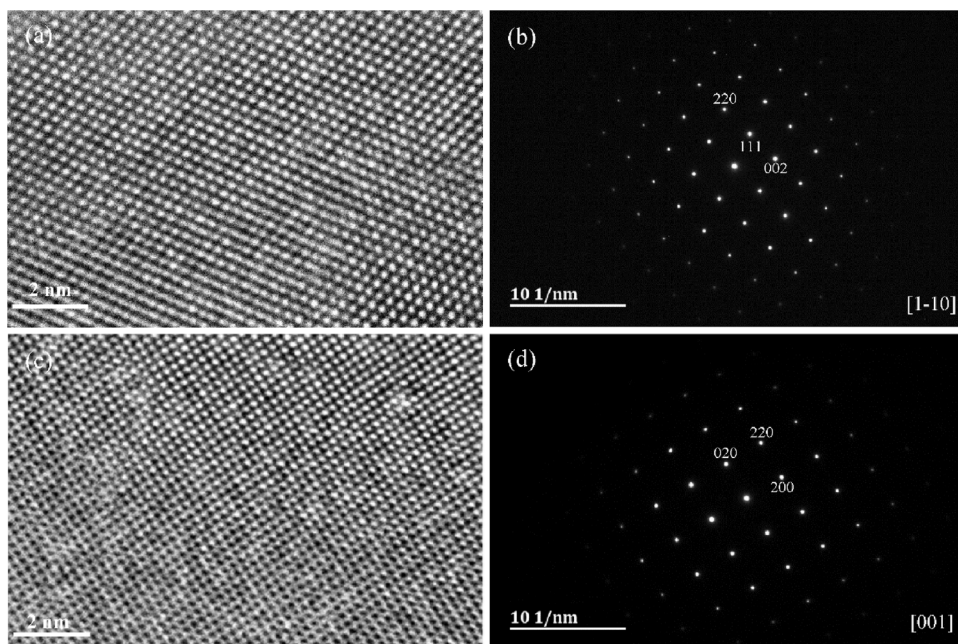


Fig. 2. HR-TEM images and corresponding SAED patterns for $(\text{Ce}_{0.2}\text{Zr}_{0.2}\text{Hf}_{0.2}\text{Sn}_{0.2}\text{Ti}_{0.2})\text{O}_2$ sample sintered at 1500 °C along the $[1\bar{1}0]$ (a, b) and $[001]$ (c, d) zone axis.

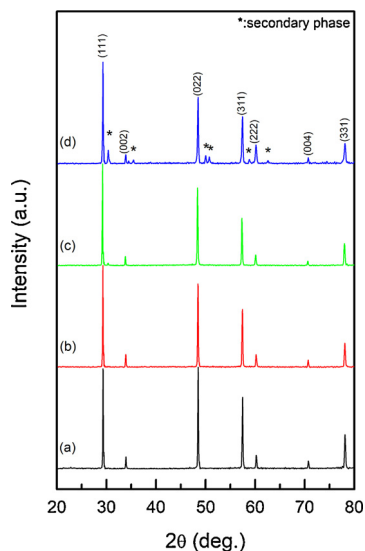


Fig. 3. XRD patterns of the samples obtained by annealing the single-phase oxide at (a) 900 °C, (b) 1000 °C, (c) 1050 °C and (d) 1100 °C for 4 h.

concentrated alloys with multi-phase microstructure have received increasing attentions due to their importance in applications [3].

We would also like to mention that the entropy-stabilized fluorite reported here is different from that reported in Ref. [11]. In the case here, all cations are equivalence of 4+, thus, no oxygen vacancies were generated during the formation of the solid solution. On the other hand, excepting Ce which is a 4-valence cation, the rest of cations are 3 valence in the material of Ref. [11]. Therefore, when forming fluorite structure, a large amount of oxygen vacancies will be generated. These vacancies can significantly increase the configurational entropy.

The electric conductivity of the obtained single-phase fluorite was measured and plot in Fig. 7. The data shows that the conductivity obey Arrhenius dependence of temperature between 600–1000 °C, suggesting that the material exhibits semiconducting behavior in this temperature range. But it deviated from Arrhenius relation at temperature higher than 1100 °C. Which is likely due to the phase separation. The data between 600–1000 °C were curve-fit to give the activation energy of 1.43 eV.

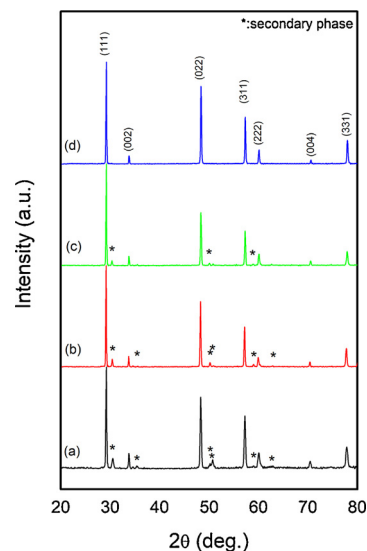


Fig. 4. XRD patterns of the samples obtained by annealing the 1100 °C and reheat treated sample at (a) 1200 °C, (b) 1300 °C, (c) 1400 °C, (d) 1500 °C for 4 h.

The room-temperature thermal conductivity of the single-phase fluorite was measured to be $1.28 \text{ W m}^{-1} \text{ K}^{-1}$. This value is only half of that for 7 wt% yttria-stabilized zirconia (7YSZ) [14]. The low thermal conductivity is likely due to the high-entropy. When the same kind of lattice position is randomly occupied by cations with different atomic radii, the lattice will be severely twisted. Which cause the decrease in the mean free path of phonon, thus the decrease in thermal conductivity. The low thermal conductivity suggests that the material could be useful for thermal insulating.

4. Conclusions

A new entropy-stabilized fluorite oxide was synthesized by sintering the equimolar mixture of CeO_2 , ZrO_2 , HfO_2 , SnO_2 , and TiO_2 . XRD analysis indicated that the obtained single-phase oxide can be transferred to a multiphase state by annealing at lower temperatures; and the multiphase state obtained by low-temperature annealing can be transferred back to the original single-phase state. The temperature for the

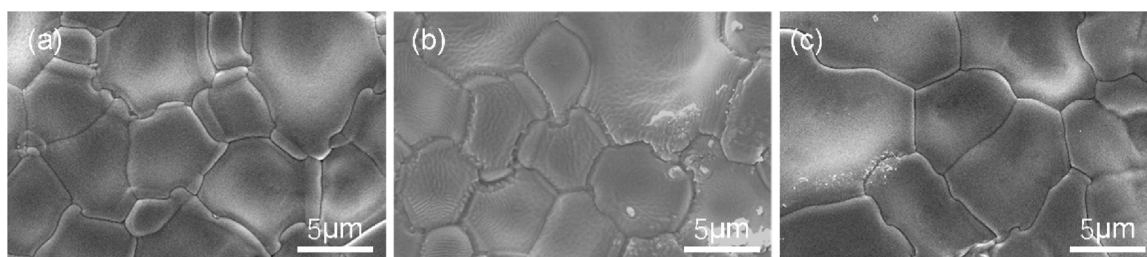


Fig. 5. SEM images of $(\text{Ce}_{0.2}\text{Zr}_{0.2}\text{Hf}_{0.2}\text{Sn}_{0.2}\text{Ti}_{0.2})\text{O}_2$ sample (a) as-sintered at 1500 °C for 6 h, (b) annealed at 1100 °C for 4 h and (c) re-heat treated at 1500 °C for 4 h.

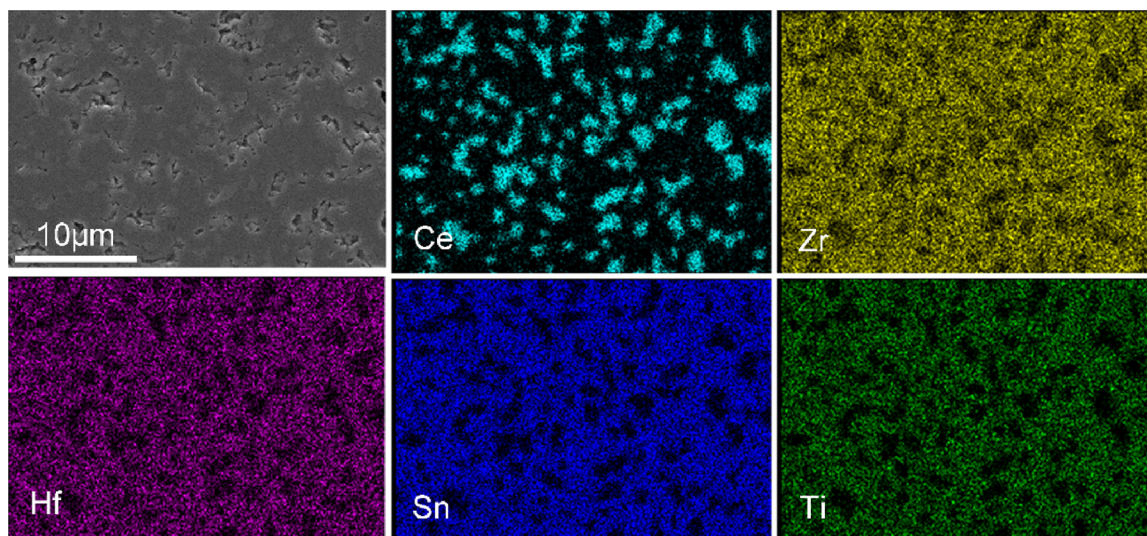


Fig. 6. Elemental mapping of $(\text{Ce}_{0.2}\text{Zr}_{0.2}\text{Hf}_{0.2}\text{Sn}_{0.2}\text{Ti}_{0.2})\text{O}_2$ sample sintered at 1500 °C for 6 h.

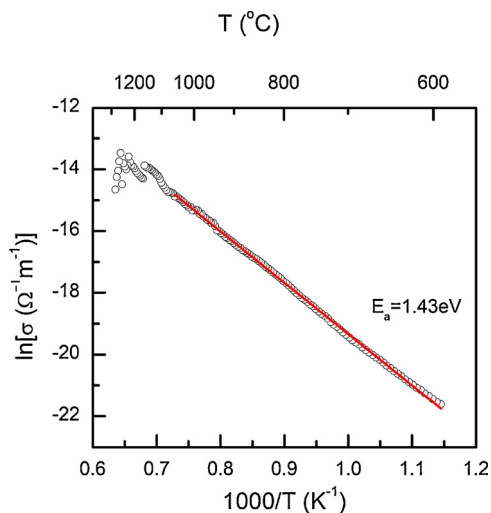


Fig. 7. The electric conductivity of the entropy-stabilized $(\text{Mg}_{0.2}\text{Co}_{0.2}\text{Ni}_{0.2}\text{Zn}_{0.2}\text{Cu}_{0.2})\text{O}_2$ as a function of temperature.

transformation between the multiphase and single-phase states is about 1500 °C. The new entropy-stabilized fluorite oxide exhibited low thermal conductivity, suggesting that it could be useful for thermal insulating applications.

Acknowledgements

The authors are grateful to Dr. Hui Wang from Beihang University and Dr. Yan Chen from Oak Ridge National Laboratory for their kind help with TEM observation and XRD Rietveld analysis, respectively.

References

- [1] J.W. Yeh, S.K. Chen, S.J. Lin, J.Y. Gan, T.S. Chin, T.T. Shun, C.H. Tsau, S.Y. Chang, Nanostructured high-entropy alloys with multiple principal elements: novel alloy design concepts and outcomes, *Adv. Eng. Mater.* 6 (5) (2004) 299–303.
- [2] B. Gludovatz, A. Hohenwarter, D. Catoor, E.H. Chang, E.P. George, R.O. Ritchie, A fracture-resistant high-entropy alloy for cryogenic applications, *Science* 345 (6201) (2014) 1153–1158.
- [3] Z. Li, K.G. Pradeep, Y. Deng, D. Raabe, C.C. Tasan, Metastable high-entropy dual-phase alloys overcome the strength–ductility trade-off, *Nature* 534 (7606) (2016) 227–230.
- [4] Y. Zhang, T.T. Zuo, Z. Tang, M.C. Gao, K.A. Dahmen, P.K. Liaw, Z.P. Lu, Microstructures and properties of high-entropy alloys, *Prog. Mater. Sci.* 61 (2014) 1–93.
- [5] M.-H. Tsai, J.-W. Yeh, High-Entropy alloys: a critical review, *Mater. Res. Lett.* 2 (3) (2014) 107–123.
- [6] D.B. Miracle, O.N. Senkov, A critical review of high entropy alloys and related concepts, *Acta Mater.* 122 (2017) 448–511.
- [7] C.M. Rost, E. Sachet, T. Borman, A. Moballeggh, E.C. Dickey, D. Hou, J.L. Jones, S. Curtarolo, J.-P. Maria, Entropy-stabilized oxides, *Nat. Commun.* 6 (1) (2015).
- [8] S. Jiang, T. Hu, J. Gild, N. Zhou, J. Nie, M. Qin, T. Harrington, K. Vecchio, J. Luo, A new class of high-entropy perovskite oxides, *Scripta Mater.* 142 (2018) 116–120.
- [9] A. Sarkar, R. Djenadic, D. Wang, C. Hein, R. Kautenburger, O. Clemens, H. Hahn, Rare earth and transition metal based entropy stabilised perovskites type oxides, *J. Eur. Ceram. Soc.* 38 (5) (2018) 2318–2327.
- [10] J. Gild, Y. Zhang, T. Harrington, S. Jiang, T. Hu, M.C. Quinn, W.M. Mellor, N. Zhou, K. Vecchio, J. Luo, High-entropy metal diborides: a new class of high-entropy materials and a new type of ultrahigh temperature ceramics, *Sci. Rep.* 6 (2016) 37946.
- [11] R. Djenadic, A. Sarkar, O. Clemens, C. Loho, M. Botros, V.S.K. Chakravadhanula, C. Kuebel, S.S. Bhattacharya, A.S. Gandhif, H. Hahn, Multicomponent equiatomic rare earth oxides, *Mater. Res. Lett.* 5 (2) (2017) 102–109.
- [12] A. Sarkar, C. Loho, L. Velasco, T. Thomas, S.S. Bhattacharya, H. Hahn, R. Djenadic, Multicomponent equiatomic rare earth oxides with a narrow band gap and associated praseodymium multivalency, *Dalton Trans.* 46 (36) (2017) 12167–12176.
- [13] J. Dąbrowa, M. Stygar, A. Mikula, A. Knapik, K. Mroczka, W. Tejchman, M. Danielewski, M. Martin, Synthesis and microstructure of the $(\text{Co,Cr,Fe,Mn,Ni})_3\text{O}_4$ high entropy oxide characterized by spinel structure, *Mater. Lett.* 216 (2018) 32–36.
- [14] J. Wu, X. Wei, N.P. Padture, P.G. Klemens, M. Gell, E. García, P. Miranzo, M.I. Osendi, Low-rare-earth zirconates for potential thermal-barrier-coating applications, *J. Am. Ceram. Soc.* 85 (12) (2002) 3031–3035.
- [15] P.H. Mayrhofer, D. Music, J.M. Schneider, Ab initio calculated binodal and spinodal of cubic Ti1-xAlxN , *Appl. Phys. Lett.* 88 (7) (2006) 071922.